Manufacturing sector - Steel Emissions Methodology

Badr Ben m'barek[1], Mason Phillpott[1] and Clément De Daniloff[1]

1) *TransitionZero*

1. Introduction

Steel production is both energy and emissions intensive, representing about 8% of total energy demand and 7% of global energy sector carbon emissions (IEA, 2020). The emissions intensity of steel production is due to its reliance on coal, the most carbon intensive fossil fuel. At the same time, steel is vitally important to the global economy, used in buildings, infrastructure, weapons, vehicles and furniture, for example. Due to its importance to modern society, steel demand is expected to grow for the foreseeable future (IEA, 2020). Steel production is also relatively centralised, with China accounting for over half of global production, followed by the European Union (EU) and United Kingdom (UK) making up 9%, India 6%, Japan 5%, the US 5%, Russia 4% and South Korea 4% (IEA, 2020).

Most importantly, steel production can be used as a proxy for emissions (i.e., kg CO_2/ton of steel) and therefore it is desirable to ascertain real time and in-depth production values to guide future climate policy. With any such globally traded commodity however, it is characterised by fierce competition amongst producers and, as a consequence, facility level production data is rarely made publicly available. In most cases it is only possible to obtain steel production/emissions quantities at the country level, and often there is a substantial delay (~years) in obtaining the data (E-PRTR contributors, 2022; UNFCCC contributors, 2022; US EPA contributors, 2022).

In this work we look to address both the temporal and spatial limitations in traditional reporting of steel production/emissions to provide more timely and accurate facility level data. More specifically, we have aimed to deliver steel production and emissions estimates on a monthly basis (with 1 month lag) for all assets identified on the Global Energy Monitor Global Steel Plant Tracker database (GEM contributors, 2022) (see section 2.1.1). Our approach improves upon certain capacity-based approaches which may only proportionately infer production between facilities or assign some average utilisation rates of installed capacities. The approach achieves this using satellite-derived mapping data which can capture variation in activity for certain types of steel facilities - and use this data to infer steel production in a given time frame.

2. Materials and Methods

During steel production, direct emissions are released during the manufacturing of crude steel, with estimates segregated by major processing routes, including blast furnace (BF), basic oxygenation furnace (BOF) and electric arc furnace (EAF). A simplified overview of the steel production value chain from raw materials to final steel products is available in Appendix 1, section 7.2.

We investigate each major processing route independently using a combination of satellite imagery, publicly reported data and academic papers. This section provides a high-level overview of the datasets and associated pipelines used to derive emission estimates for the iron and steel sub-sector.

Given the lack of asset-level emission data publicly available, a standardised "bottom-up" approach is used to quantify the emissions. This process is characterised by first estimating production levels for each plant (in tons of crude steel produced for a steel plant, for instance) before then subsequently applying a calculated emissions factor (tons of CO_2 per ton of crude steel produced) to generate emissions estimates.

There are primarily two approaches to estimating asset level production. As a priority, satellite-derived production estimates are used whenever a facility releases enough heat to be captured by satellite imagery (Zhou *et al.*, 2018; Marchese *et al.*, 2019; Liangrocapart, Khetkeeree and Petchthaweetham, 2020). This is the case for BF-BOF facilities which have several units that function at temperatures higher than 1,200^{o}C. These hotspots include signals from coke plants, sinter plants, BFs, slag pits, and BOFs (Figure 2). For all the other plants where hotspots were not captured on satellite imagery (steel via EAF for instance), we used a basic disaggregation method. This is determined by calculating each plant's share of national capacity, before multiplying this number by the country's production to derive the plant's contribution for the given timeframe. For country-level statistics these point-source estimates are then aggregated. Figure 1 summarises the modelling approach, however, M'Barek and Gray (2021) provide a more detailed methodological breakdown.

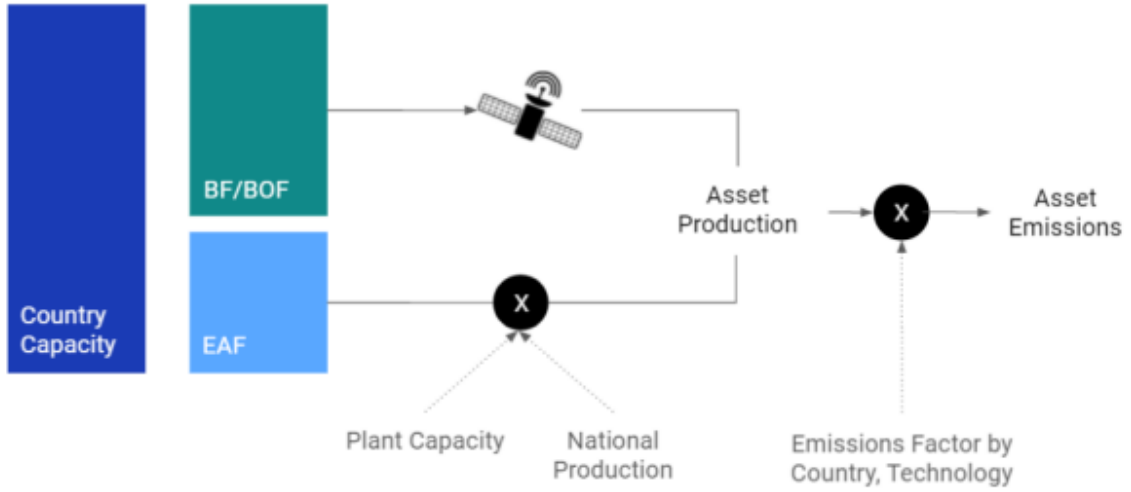

Figure 1 Example of the modelling approach to quantify asset-level emissions for the Iron & Steel industry, segregated by steel processing route.

2.1. Materials

2.1.1. Asset inventory dataset

Global Energy Monitor (GEM) provides facility level information such as GPS coordinates, owner, capacity, age, product type and technology type. Through the Global Steel Plant Tracker initiative (GSPT) data is available for all plants meeting the 0.5 million metric tons per annum (Mt/a) threshold that have been proposed since 2017 or retired or mothballed since 2020 (GEM, 2022). In total there are 861 unique steel facilities with an annual production capacity of 2,345 Mt across 78 countries. Since we use remote sensing data, we need facility geolocation data accurate to within a few tens of metres. While some of the listed geolocation from the GEM dataset provides geolocation information, it is in some cases, approximative. We supplement the source geolocation data using the Google Maps API (Google Maps, 2022) and OpenStreetMap (OpenStreetMap, 2022), before manually validating all geolocations. Figure 2 shows how steel assets are distributed globally with high concentration of assets in China followed more distantly by the US, India and Japan (facility count details in section 7.5 Appendix 4, Table 2 and 3). The map also highlights countries with little to no steel production, mainly concentrated in Sub-Saharan Africa, Latin America and Southeast Asia.

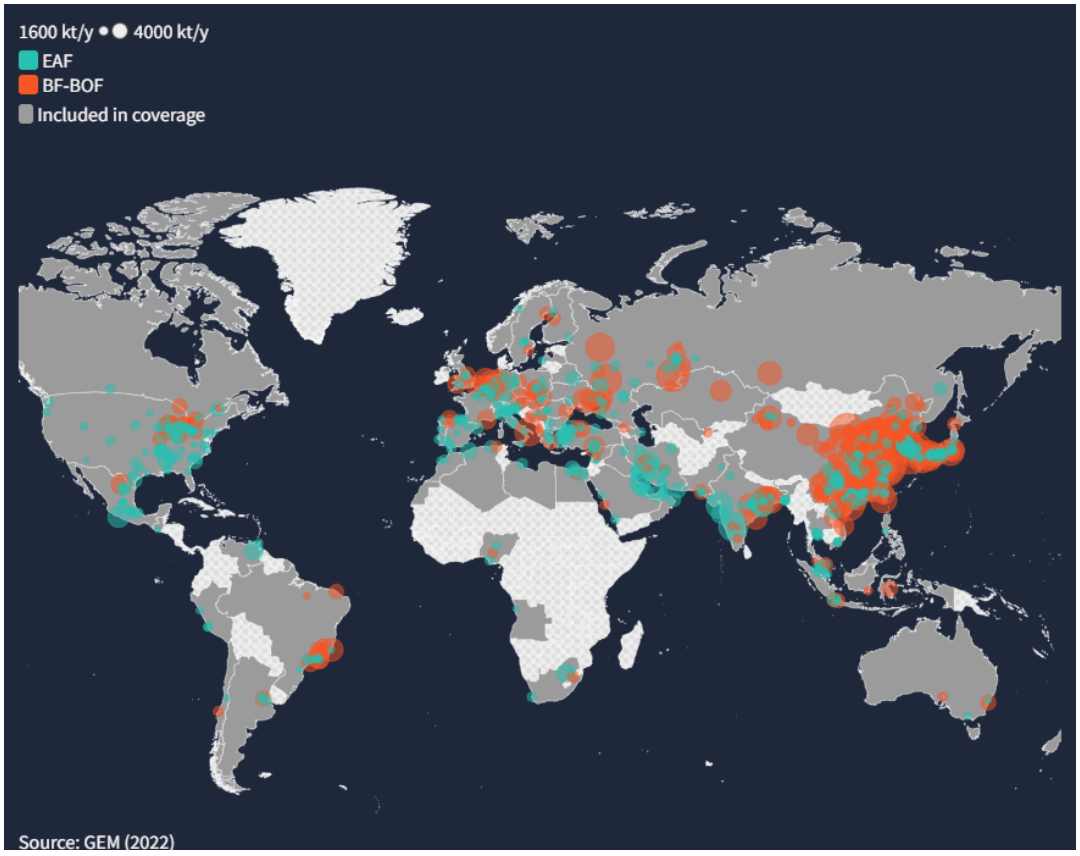

Figure 2 Global map showing steel facilities. Countries included in steel emissions monitoring are shaded with EAF (green) and BF-BOF (orange) major processing routes identified.

2.1.2. Remote sensing datasets

Satellite based production estimates make use of multispectral image from two different collections:

- The European Space Agency (ESA) Copernicus Sentinel mission with a resolution of 20m and a combined 5-day at the equator revisit with two satellites:
    - Sentinel 2A: with historical images available since 2017 (ESA, 2022).
    - Sentinel 2B: with historical images available since 2017 (ESA, 2022).
- The U.S. Geological Survey (USGS) and National Aeronautics and Space Administration (NASA) Landsat program with a resolution of 30m and a combined 8-day revisit:
    - Landsat-8: with historical images available since 2015 (NASA and USGS, 2022a).
    - Landsat-9: with historical images available from 2022 (NASA and USGS, 2022b).

All images are sourced and processed using Google Earth Engine (Google Earth Engine, 2022a, 2022b, 2022c). For each image, we rely on the surface reflectance product and compute the normalised band ratio between the two short wave infrared bands of each satellite, called the

Normalised Heat Index (NHI). For the respective satellite collections, we infer the NHI through the following calculations:

- Sentinel-2A/B: $NHI = \frac{(B12 - B11)}{(B12 + B11)}$
- Landsat-8/9: $NHI = \frac{(B07 - B06)}{(B07 + B06)}$

Where B# refers to the band number for the specific satellite. This ratio is used to identify thermal anomalies within the temperature range of industrial processes, while eliminating most of the noise from reflectance interference (adapted from Kato (2021) for industrial applications). Pixel values between the Sentinel 2A/B MultiSpectral Instrument and Landsat Operational Land Imager Instrument were harmonised using NASA's band pass adjustments (NASA, 2018), allowing the two image collections to be used as if they were a single collection. The harmonised dataset ensured higher revisit for time-series surface applications. Partial images (coverage of the facility's boundaries less than 80%) and cloudy images (more than 20% clouds) are excluded. Figure 3 shows an example of NHI with identified hotspot locations at a steel plant.

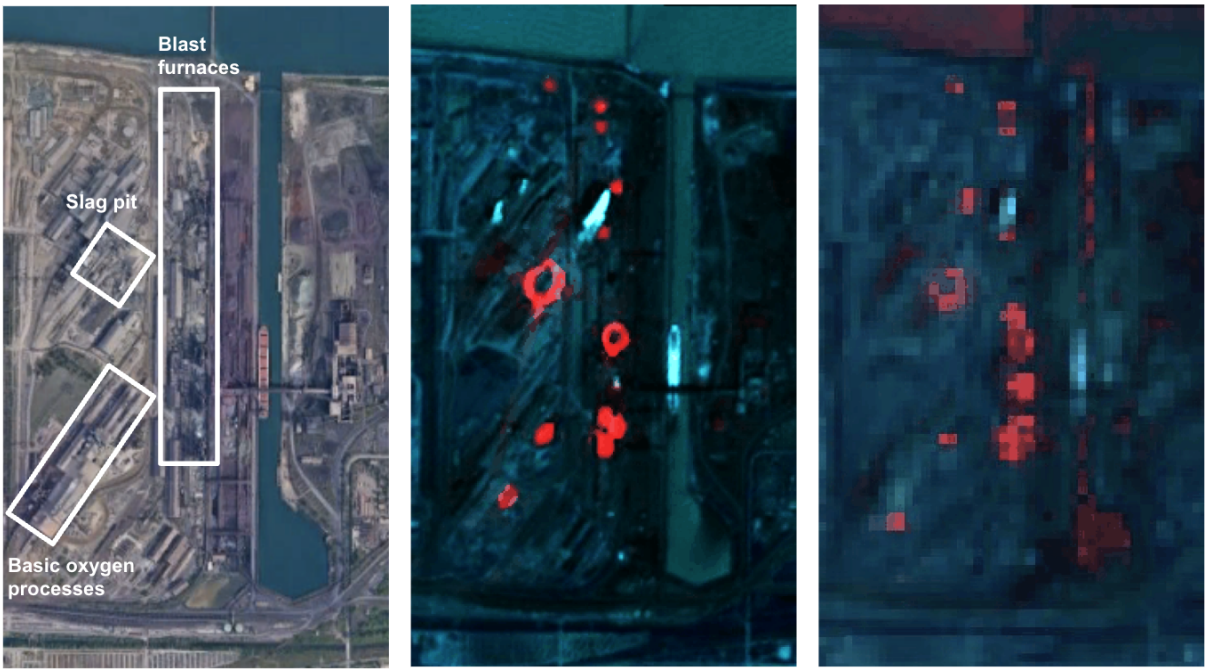

Figure 3 Left - high resolution image of Gary Steel plant, (U.S.A), overlaid with manual labelling of major heat-releasing units; Middle - composite Sentinel-2 image acquired on May 30th, 2021, using the NHI which shows thermal anomalies (red for hot pixels, blue for cooler pixels); Right - composite Landsat 8/9 image acquired the same day, also using the NHI to show thermal anomalies. Sources: modified Copernicus and USGS data, OpenStreetMap, and Terrametrics.

2.1.3. Production datasets

Aggregated steel production used in our models is primarily sourced from Worldsteel (Worldsteel, 2022) for national statistics, except for China, where more granular province level data is available through the Chinese National Bureau of Statistics (CNBS) (CNBS, 2022). This improved spatial granularity in China is particularly critical to improve modelling granularity as China accounts for approximately half of the global capacity at 1,170 Mt/a with 341 assets available in the GEM database. All aggregated production statistics are sourced on a monthly basis. In a select few countries, such as Albania, Morocco and North Korea, only annual production data were available and monthly level data were approximated through disaggregation of these values. All countries and provinces demonstrate production values for the period starting January 2015. Lastly, in 12 countries, production data were available however there were no assets associated with the given geography. This temporal and spatial mismatch likely occurs due to limitations in the GEM database which currently only has records on assets with capacity higher than 0.5 Mt/a. Future updates to this database may look to include smaller assets.

2.1.4. Emissions factors dataset

Emissions factors from Global Efficiency Intelligence (GEI contributors, 2022) are provided by steel processing route and country, and these are used to convert facility level production estimates to emissions. Countries include Brazil, Canada, China, France, Germany, India, Italy, Japan, Mexico, Poland, Russia, South Korea, Spain, Turkey, Ukraine, United States, and Vietnam. For other countries we used the median emission factor by production process. Use of the median emissions factor was preferable in this case to avoid bias through the inclusion of extreme values demonstrated in some countries. Power generation related emissions are excluded from these emission factors (when applicable) as these emissions are already accounted for in the Climate TRACE Electricity generation sector.

2.1.5. Validation datasets

In this work facility level production and emissions models are developed based upon country-level target data. As a consequence, alternative sources are required to validate our model results. Our results are validated against both production and emissions. In some cases, the GEM database provides crude steel production values in addition to asset inventory data. Most often these values extend only to the most recent year (i.e., 2020). To supplement these records, we have obtained production data from other freely available online sources (AIST contributors, 2022; BlueScope Illawarra contributors, 2022; GMK centre contributors, 2022). For emissions, globally, only the US Environmental Protection Agency (US EPA) and the European Pollutant Release and Transfer Register (E-PRTR) publish facility level data (E-PRTR, 2022; US EPA, 2022). In this work both sets of these values are recorded on an annual basis and are utilised as a benchmark to validate the performance of our own model estimates.

2.2. Methods

2.2.1. Production methodology

The first step to quantifying emissions for each steel asset is estimating the associated activity, expressed in tons of crude steel produced in a given time period. We rely on three modelling methods to estimate individual production levels, with more details given in the following sections. An example of the resulting country-level coverage of steel production by modelling method is available in Appendix 3.

2.2.1.1. Satellite-derived estimates

At BF-BOF steel plants, once hotspot activities were identified from the satellite NHIs, country level production data was used to calibrate the relationships between these activities and production at the plant level, visualised in Figure 4. Specifically, we begin by extracting the shapes of all hotspots at each plant. For each of these hotspots, a time-series of pixel values was extracted before signal processing was applied to normalise these values between zero and one (Figure 9 in Appendix 2). Each normalised hotspot time-series was fed into an optimizer function which developed a linear relationship (or weight) between hotspot NHI and reported country level production. Model constraints were also implemented during this optimization phase that ensured individual plant predictions should not exceed their maximum capacity. The asset production estimates were then back calculated using the asset's hotspot signals and their corresponding weight.

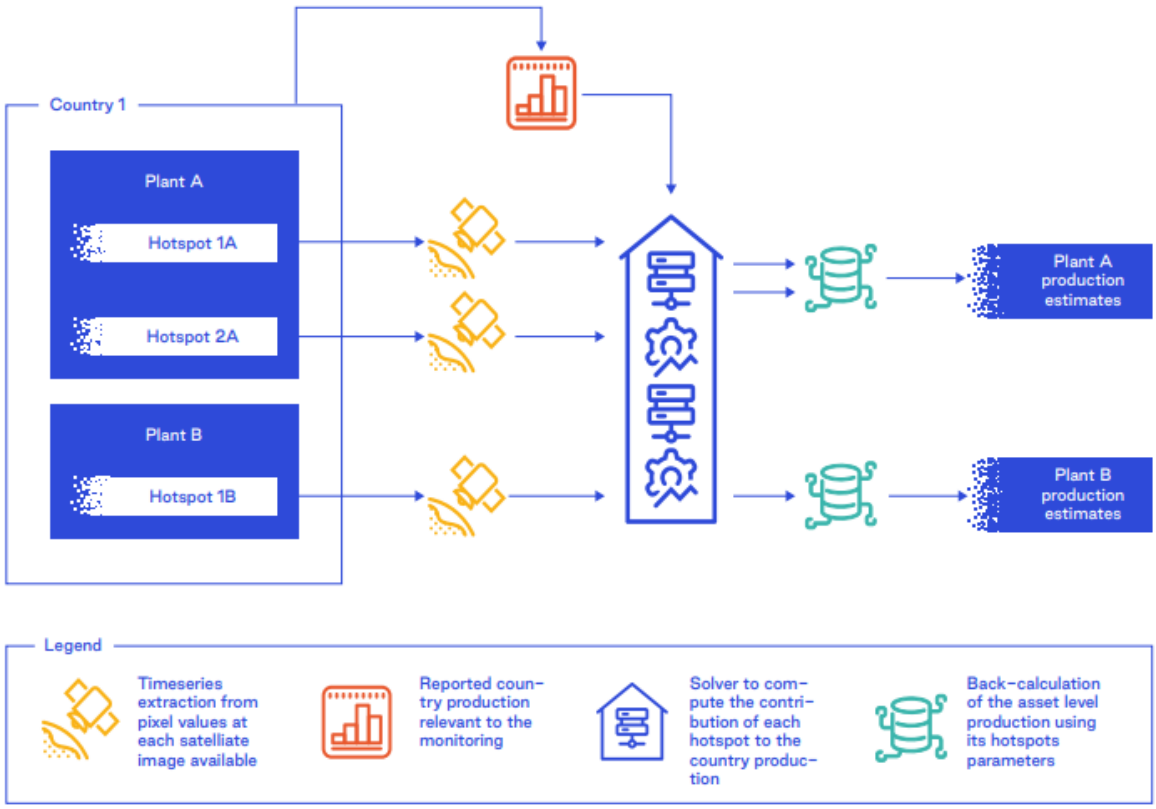

Figure 4 Schematic model approach for satellite-based estimates of facility level production.

An illustrative example of the satellite processing steps is highlighted in Appendix 2.

2.2.1.2. Capacity-based estimates

For assets which are not monitored via satellite (i.e., EAF steel production), a basic disaggregation method is applied: for each facility, we compute its share of national capacity, before multiplying this number by the country's remaining production (after accounting for satellite-derived asset production estimates) to derive the facility's contribution for the given timeframe. An illustrative example of a country with two plants A and B (of capacities C_A and C_B respectively) and a total production P_m for a country/region and a given month m, the capacity-based estimates for these two plants are (respectively $P_{A,m}$ and $P_{B,m}$):

- $P_{A,m} = \frac{C_A}{C_A + C_B} \times P_m$
- $P_{B,m} = \frac{C_B}{C_A + C_B} \times P_m$

2.2.1.3. Non-spatially allocated asset estimates

In some cases, there is a shortfall between the sum of satellite and capacity-based asset production estimates and the country-level production targets. This circumstance may occur when the capacity of listed assets is lower than the aggregated production figures (country or province-level). This missing production is then allocated to a non-spatially allocated asset for the purposes of more accurately estimating country-level emissions.

2.2.2. Emissions methodology

With the production estimates derived for each asset, the emission estimates were derived by multiplying the production by the relevant emission factor (Hasanbeigi, 2022). Energy-related emissions were excluded from these emission factors (when applicable) as these emissions are already accounted for in other parts of the Climate TRACE Electricity generation sector. For non-spatially allocated asset production, the average emissions factor for a country was used and weighted by the share of processing capacity of each route within the country.

2.3. Coverage

Based on 2021 production numbers, asset level estimates for 82% (1934 Mt/a) of world crude steel production are provided. The remaining 18% are provided through the country level estimates as non-spatially allocated assets. While satellite-monitored assets only represent 37% of total assets (321 out of 861), these assets contribute to 83% of the total asset level emissions estimates (1,740 out of 2,107 $MtCO_2$/a) in 2021. A more detailed breakdown of coverage is available in Table 2 and 3 in section 7.5 Appendix 4.

3. Results and analysis

Our methodology provides production and, by extension, emissions estimates at a monthly level. In this section our results are provided through statistical analysis. Accuracy is assessed by first gathering production and emissions data for assets before then subsequently calculating median of absolute errors (MAE) and median of absolute percentage errors (MAPE) statistics across data. The results section consists of four subsections that explore how our modelled production and emissions estimates compare to external sources: steel production (Section 3.1), steel emissions (Section 3.2), emissions factor analysis (Section 3.3), and aggregated steel emissions (Section 3.4).

3.1. Comparison of asset level production estimates

Initially, the accuracy of the production estimates at the asset level is addressed. Unlike country-level production, asset level production is not easily accessible and is only available for select countries or facilities. Furthermore, values are only found documented at annual

production rates. In total there are 251 facilities yielding 460 samples available for comparison with modelled estimates (sources listed in Section 2.1.5). Figure 5 shows the results of this work where asset level production estimates are compared to known production targets for a given year. Overall, MAE (MAPE) accuracy across the total number of measurements, otherwise referred to as samples, is 0.36 Mt/a (18%). Within the figure the plant types are split according to their estimation method with 114 capacity-based assets (189 samples) and 137 satellite-based assets (271 samples). For these groups an accuracy of 0.20 Mt/a (23%) and 0.54 Mt/a (16%) is observed, respectively. Satellite-based assets, consisting of BF-BOF facilities tend to be substantially larger than the capacity (mostly EAF) based counterparts, and, as such, comparison of absolute percentage errors is more representative of model performance. In this case it is observed that, on average, asset production which is estimated by satellite is up to 7% more accurate than those estimated through the capacity-based production approach.

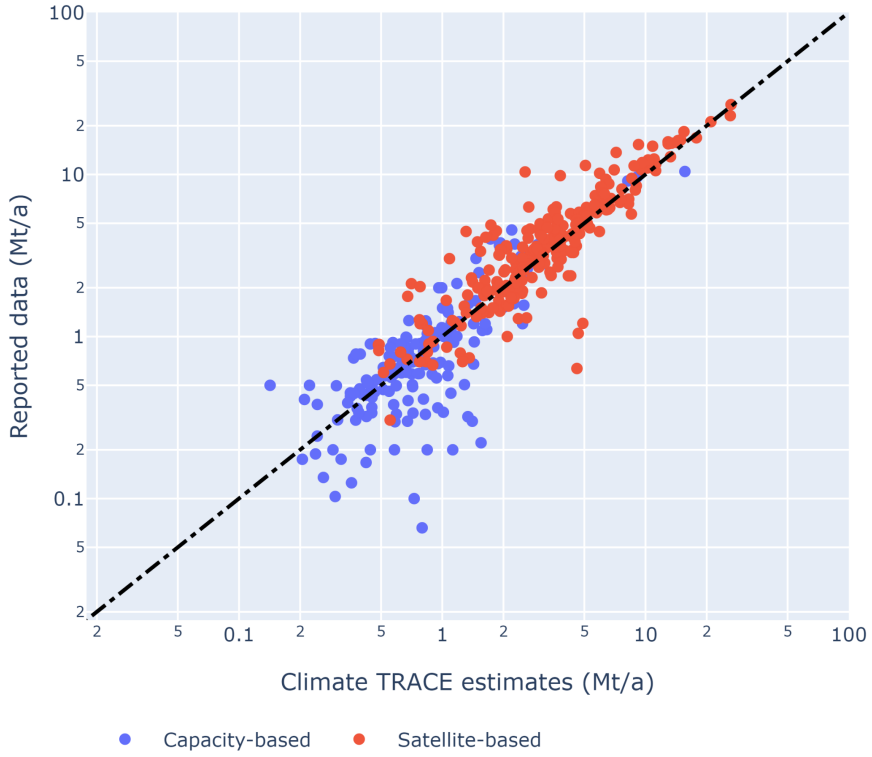

Figure 5 Comparison of asset level production estimates to known target values across periods January 2015 to December 2021. Red dots = satellite-based production estimates, blue-dots = capacity-based estimates. Axes expressed in log-scale.

3.2. Comparison of asset level emissions estimates

In this section our CO_2 emissions estimates are compared to reported data by the US EPA and E-PRTR (US EPA, 2022; E-PRTR, 2022). Data is published at an annual resolution in both cases, so our own monthly emissions estimates will be aggregated on an annual basis for comparison.

The results of this analysis are displayed in Figure 6. In total there are 118 assets (565 samples) of which 51 are from the EU (178 samples) and 67 from the US (390 samples). Overall, MAE (MAPE) accuracy across the samples is 0.08 $MtCO_2/a$ (31%). Of the 118 assets, 90 are capacity based (441 samples) and 28 are satellite-based (124 samples) with accuracy of 0.05 $MtCO_2/a$ (31%) and 1.01 $MtCO_2/a$ (26%), respectively. Here a lower emissions factor in combination with generally smaller capacity for capacity-based assets results in a substantially lower MAE. By comparing for MAPE however it is seen that the satellite-based approach is 5% more accurate on average.

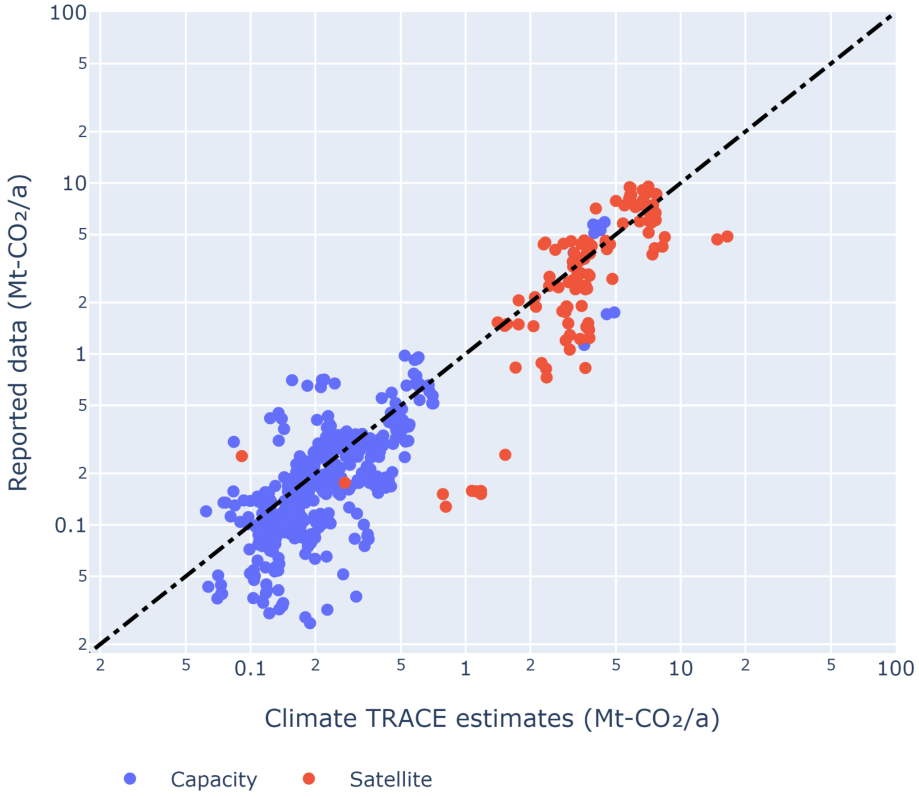

Figure 6 Comparison of asset level CO_2 emissions estimates to reported estimates from the US-EPA and E-PRTR for periods January 2015 to December 2021. Red dots = satellite-based production estimates, blue dots = capacity-based estimates.

3.3. Analysis of emissions factors

There are 22 assets which share both production target and emissions data for the same year(s). In total this yields 55 samples that are available for comparison. The results of this analysis are shown in Appendix 5 Table 4 which indicates the average accuracy results for each asset in addition to the capacity, main production process and the implied emissions factor. The implied emissions factor is calculated directly through the known annual production and emissions, as listed in their relevant source (for example, a company report) and US EPA/E-PRTR

respectively. In three cases the MAPE exceeds 30% for production, all of which are relatively small (0.8-1.11 Mt/a) EAF assets from the US. The lower accuracy for the EAF assets is not unexpected and is likely due to the methodology used in these cases. The US for instance has 72 total assets, however only 9 (12%) of these assets are monitored by satellite (Table 2). Capacity-based estimates are completed on the remaining 61 (88%) of assets. For such a large ratio of capacity-based assets the assumption of proportional production is unlikely to be accurate in all cases. For emissions estimates there are 10 assets where MAPE exceeds 30%. One of these cases, the 1 Mt/a EAF plant Cleveland-Cliffs Steelton LLC (GEM ID SUS00008), can be explained due to the inaccurate production estimate which is proportionately linked to the emissions value (via the facility type and country specific emissions factor). For the remaining nine assets we show that the implied emissions factor differs from our own.

3.4. Aggregated emissions estimates for EU, US

Asset level emissions estimates are the target of this work. However, it is also useful to validate our results at a more aggregated level. Figure 7 highlights the results based on aggregated annually reported emissions for selected plants (as stated in Section 3.2) in the EU and US, respectively. In both cases our results capture the overall trend of emissions in each region. For the EU our own estimates are more accurate in the last 2-3 years relative to earlier years and converge closely upon the later reported figures. For the US, our emissions estimate closely reflect the trend of reported emissions throughout the monitoring period. The MAE (MAPE) for 2015 to 2020 is 7.31 $MtCO_2/a$ (15%) and 1.10 $MtCO_2/a$ (3%) for the EU and US, respectively.

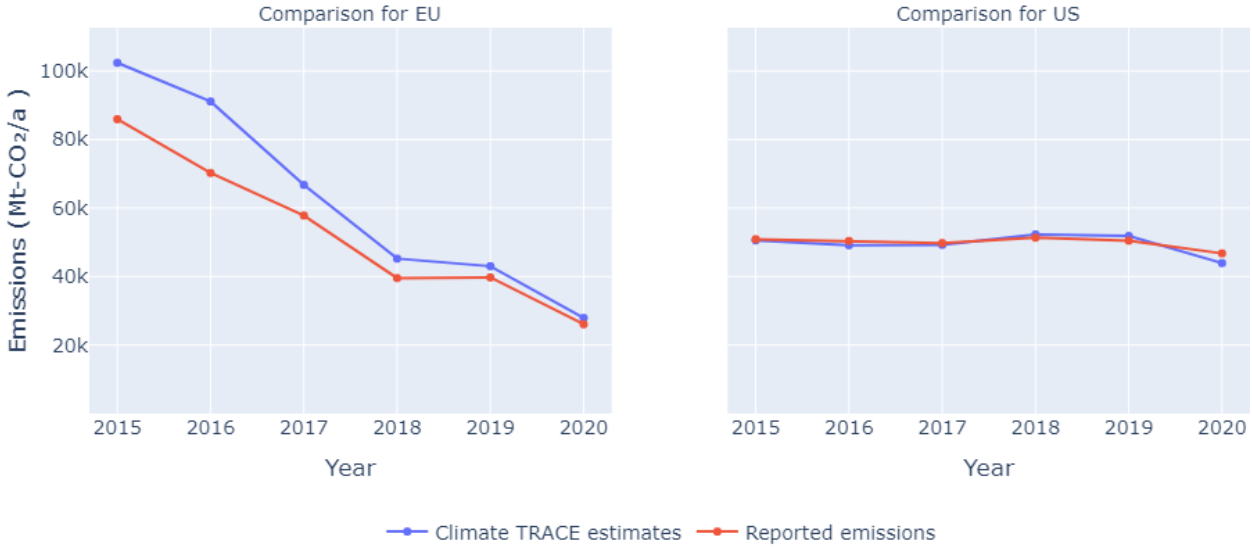

Figure 7 Comparison of reported emissions and Climate TRACE emissions estimates for the EU (left) and US (right).

4. Discussions

Our steel emissions estimates modelling approach consists of first, estimating facility level production, and second, applying a relevant emissions factor to yield facility emissions. The approach for estimating steel production at the facility level is dependent upon the facility type. BF-BOF facilities are estimated via our satellite-based approach as they contain numerous elements such as the coke plants, sinter plants, BFs, slag pits, and BOFs which can operate at temperatures in excess of 1,200ºC. Such high temperatures present a strong signal which can be used as a proxy for inferring activity (or production) for a given facility at a given time. Other facilities that do not present such high temperature elements, such as EAF type facilities, are instead estimated via the capacity-based approach. The satellite-based approach is advantageous in that it can provide an estimation of dynamic activity that more realistically represents the facility itself as opposed to the capacity-based approach which reflects national production. A comparison of the two approaches shows results to this effect- satellite-based production estimates a MAPE of 16%, which is 7% greater than the average capacity-based facility. Such an improvement in accuracy for the BF-BOF type facilities is important in global emissions estimates due to their generally larger capacity and higher emissions factor that results in a considerably higher contribution to global emissions. Limitations in this approach may arise from either the incorrect detection of relevant hotspots or lack of enough training data. In both cases a larger study period is expected to improve the accuracy our model estimates.

Following our production estimates, country or region-specific emissions factors are used for each facility type to estimate facility level emissions. These emissions estimates are the main goal of this work. Our results show a MAE (MAPE) accuracy of 0.08 $MtCO_2/a$ (31%) across 118 assets and 7.31 $MtCO_2/a$ (15%) and 1.10 $MtCO_2/a$ (3%) for the aggregated emissions across EU and US, respectively. Overall accuracy is generally strong, however, was reduced due to a select few cases which did not perform well under the given methodology. Either providing emissions estimates which were too large or small when compared to the reported figures. For 22 facilities we had access to both production and emissions reported figures which presented an opportunity to investigate some of these cases. Three main hypotheses are presented for differences in emissions estimates: (1) different reporting scope, (2) country/region specific emissions factors, (3) poor production estimates, and there could additionally be many causes for these discrepancies for which it is not always trivial to identify in each facility. A difference in reporting scope of the emissions between the reported data and the emission factors is suspected in some cases. In our own models we looked to compare direct emissions, however, reported values were not always clear on their exact scope. An example may be that a specific facility would include the associated emissions of electricity in addition to those released through production of steel which would differ from our own. Another reason can be linked to the fact that the emission factors we use are country and production method specific. For countries with numerous facilities these values may not always be representative for each plant. Emissions

intensity is likely to vary substantially based upon the age of the facility, fuel mix, feedstocks and use of energy-efficient technologies, for example (Hasanbeigi, 2022). Lastly, our production estimates may themselves be incorrect and, as emissions are directly proportional, would result in poor estimates for the emissions themselves. A case here would be for a capacity-based facility which is not producing consistently with the national average and would therefore not be represented well.

More work could be done to improve these estimates given a more granular reference production data set to be used in training of facility level models. For example, each facility estimate is currently based upon models trained relative to country level production data. If facility level production data were available (at scale), model complexity would decrease in line with more representative target data and greater accuracy could be achieved. Such a process would only be required for model development and once calibrated, could provide up-to-date estimates with little work on the part of data collection. Secondly, to improve emissions estimates a natural improvement in accuracy would follow if facility-specific emissions factors were available in contrast to the national/regional values used currently. This second improvement will be the focus of future iterations on this work. Lastly, while we provide production and emissions estimates to all assets reported by the GEM steel tracker tool, it is not a complete set of global facilities (China for instance). As GEM aims to include more assets in its own database (i.e., assets with <500Mt/a) we will aim to provide an update accordingly.

5. Conclusion

In this work a new approach has been implemented to estimate steel production and emissions at a facility level and on a monthly basis for all 861 steel plant assets, covering 78 countries, in the GEM database. In total these assets cover 82% (1,609 out of 1,952 Mt/a) of worldwide crude steel production.

This steel production methodology was dependent on facility type, BF-BOF and EAF. Facilities with strong heat signatures, such as BF-BOF processing routes, were approximated using satellite-derived NHI measurements. Such an approach allowed for the use of machine learning to infer a relationship between facility hotspots and steel production - ultimately resulting in more accurate and timely estimates. For facilities where steel processing routes did not provide useful satellite information, such as EAF, a capacity-based approach was used to infer production estimates. Based on the 2021 production numbers, our satellite-monitored assets account for only 37% of total assets, however, contribute 83% of total asset CO_2 emissions (1,740 out of 2,107 $MtCO_2/a$). Comparing capacity and satellite-based production estimates to reported values, there is marked improvement of 7% MAPE in accuracy for satellite-based assets. Overall, MAE (MAPE) accuracy was at 0.36 Mt/a (18%) for all samples. The remaining 18% of production not

accounted for belonged to small assets (<0.5 Mt/a) which, for the purpose of estimating emissions at the country level, were introduced as non-spatially allocated assets.

To calculate emissions, we applied country and process-specific emission factors (Hasanbeigi, 2022) to our production estimates which were subsequently compared to reported facility and country-level figures. This analysis yielded a MAE (MAPE) accuracy of 0.08 $MtCO_2$/a (31%) across 118 assets and 7.31 $MtCO_2$/a (15%) and 1.10 $MtCO_2$/a (3%) for the aggregated emissions across EU and US, respectively. Lastly, for a few assets (22) it was possible to correspond reported production and emissions on a given year. Through these instances we extracted an implied emissions factor which could be used to verify our own cited source and validate its usefulness. We noted strong production accuracy across the assets (19/22 assets, <30% MAPE), however fewer assets met the same criteria for emissions (12/22 assets, <30% MAPE). These results show that our methods are effective at estimating steel production, and emissions in most cases. The few cases with lower emissions accuracy highlight that a wide variation in emissions factors may be present for a given facility within a country which may not necessarily be fully captured by just process type alone. For example, 8 out of the 10 assets belonged to the US with 72 assets of varying age, fuels, and technologies.

Ultimately, this work has shown that timely and accurate facility level production and emissions can be obtained without the need to rely upon factory published figures, often years out of date, and may open pathways to assist in future climate policy. Future works may benefit from greater availability of asset data to train in modelling, allowing subsequent versions of our model to benefit from a greater scope of historical data that may further improve our model results. Furthermore, as GEM begins to target smaller assets for inclusion in their database, we will be able to update our own results accordingly.

6. References

1. AIST contributors (2022) ‘Steel production data retrieved from: AIST’. Association of Iron and Steel Technology (AIST).
2. Bluescope Illawarra contributors (2022) ‘Steel production data retrieved from: Bluescope Illawarra’. Bluescope Illawarra. Available at: https://www.bluescopeillawarra.com.au/.
3. CNBS contributors (2022) ‘Steel production data retrieved from: CNBS’. China National Bureau of Statistics (CNBS). Available at: http://www.stats.gov.cn/english/.
4. E-PRTR contributors (2022) ‘Steel emissions data retrieved from: E-PRTR’. European Pollutant Release and Transfer Register (E-PRTR). Available at: http://prtr.ec.europa.eu/.
5. European Space Agency (ESA) (2022) ‘Satellite images data retrieved from: Copernicus Sentinel-2 ESA’. Available at: https://www.esa.int/Applications/Observing_the_Earth/Copernicus/Sentinel-2.
6. GEI contributors (2022) ‘Steel emission factor data retrieved from: GEI’. Global Efficiency Intelligence (GEI). Available at: https://www.globalefficiencyintel.com/.

7. GEM contributors (2022) ‘Steel inventory data retrieved from: GEM Global Steel Plant Tracker’. Global Energy Monitor (GEM). Available at: https://globalenergymonitor.org/projects/global-steel-plant-tracker/.
8. GMK centre contributors (2022) ‘Steel production data retrieved from: GMK centre’. GMK centre. Available at: https://gmk.center/en/.
9. Google Earth Engine (2022a) *Landsat 8 Datasets in Earth Engine*, *Google Developers*. Available at: https://developers.google.com/earth-engine/datasets/catalog/landsat-8 (Accessed: 26 July 2022).
10. Google Earth Engine (2022b) *Landsat 9 Datasets in Earth Engine*, *Google Developers*. Available at: https://developers.google.com/earth-engine/datasets/catalog/landsat-9 (Accessed: 26 July 2022).
11. Google Earth Engine (2022c) *Sentinel-2 Datasets in Earth Engine*, *Google Developers*. Available at: https://developers.google.com/earth-engine/datasets/catalog/sentinel-2 (Accessed: 26 July 2022).
12. Google Maps contributors (2022) ‘Steel inventory data retrieved from: Google Maps’. Google. Available at: https://www.google.co.uk/maps.
13. Hasanbeigi, A. (2022) ‘An International Benchmarking of Energy and CO2 Intensities’, p. 31.
14. IEA (2020) ‘Iron and Steel Technology Roadmap - Towards more sustainable steelmaking’, p. 190.
15. Kato, S. (2021) *Automated classification of heat sources detected using SWIR remote sensing | Elsevier Enhanced Reader*. Available at: https://doi.org/10.1016/j.jag.2021.102491.
16. Liangrocapart, S., Khetkeeree, S. and Petchthaweetham, B. (2020) ‘Thermal Anomaly Level Algorithm for Active Fire Mapping by Means of Sentinel-2 Data’, in *2020 17th International Conference on Electrical Engineering/Electronics, Computer, Telecommunications and Information Technology (ECTI-CON)*. *2020 17th International Conference on Electrical Engineering/Electronics, Computer, Telecommunications and Information Technology (ECTI-CON)*, pp. 687–690. Available at: https://doi.org/10.1109/ECTI-CON49241.2020.9158262.
17. Marchese, F. *et al.* (2019) ‘A Multi-Channel Algorithm for Mapping Volcanic Thermal Anomalies by Means of Sentinel-2 MSI and Landsat-8 OLI Data’, *Remote Sensing*, 11(23), p. 2876. Available at: https://doi.org/10.3390/rs11232876.
18. M’Barek, B. and Gray, M. (2021) ‘The Spotlight Effect’. Transition Zero. Available at: https://www.transitionzero.org/reports/the-spotlight-effect.
19. National Aeronautics and Space Administration (NASA) (2018) ‘Band Pass Adjustment’. Available at: https://hls.gsfc.nasa.gov/algorithms/bandpass-adjustment/ (Accessed: 25 July 2022).
20. National Aeronautics and Space Administration (NASA) and United States Geological Survey (USGS) (2022a) ‘Satellite images data retrieved from: Landsat-8 NASA/USGS’. Available at: https://www.usgs.gov/landsat-missions/landsat-8.

21. National Aeronautics and Space Administration (NASA) and United States Geological Survey (USGS) (2022b) ‘Satellite images data retrieved from: Landsat-9 NASA/USGS’. Available at: https://www.usgs.gov/landsat-missions/landsat-9.
22. OpenStreetMap contributors (2022) ‘Steel inventory data retrieved from: OpenStreetMap’. OpenStreetMap. Available at: https://www.openstreetmap.org/.
23. UNFCCC contributors (2022) ‘Steel emissions data retrieved from: UNFCCC’. United Nations Framework Convention on Climate Change (UNFCCC). Available at: https://unfccc.int/process-and-meetings/transparency-and-reporting/greenhouse-gas-data/ghg-data-unfccc/ghg-data-from-unfccc.
24. US EPA contributors (2022) ‘Steel emissions data retrieved from: US EPA’. United States Environmental Protection Agency (US EPA). Available at: https://www.epa.gov/.
25. Worldsteel contributors (2022) ‘Steel production data retrieved from: Worldsteel’. Worldsteel. Available at: https://worldsteel.org/.
26. Zhou, Y. *et al.* (2018) ‘A Method for Monitoring Iron and Steel Factory Economic Activity Based on Satellites’, *Sustainability*, 10(6), p. 1935. Available at: https://doi.org/10.3390/su10061935.

7. Appendices

7.1. List of acronyms

Table 1 List of acronyms.

BF	blast furnace
BOF	basic oxygen furnace
CNBS	China National Bureau of Statistics
CO_2	carbon dioxide
E-PRTR	European Pollutant Release and Transfer Register
EAF	electric arc furnace
GEI	Global Efficiency Intelligence
GEM	Global Energy Monitor
GSPT	Global Steel Plant Tracker initiative
IEA	International Energy Agency
MAE	median of absolute errors
MAPE	median of absolute percentage errors
Mt	million metric ton
NASA	National Aeronautics and Space Administration
NHI	Normalised Heat Index
US EPA	United States Environmental Protection Agency
USGS	United States Geological Survey
Worldsteel	World Steel Association

7.2. Appendix 1: Overview of the steel production process

The principal inputs to steelmaking today are iron ore, energy, limestone and scrap. Iron ore and scrap are used to provide the metallic charge, with scrap having a much higher metallic concentration than iron ore. Energy inputs are used to provide heat to melt the metallic input, and in the case of iron ore, to chemically remove oxygen. Limestone is used at various stages of the steelmaking process to help remove impurities. Indirect carbon emissions vary widely based on the production route. Figure 8 highlights these main process routes.

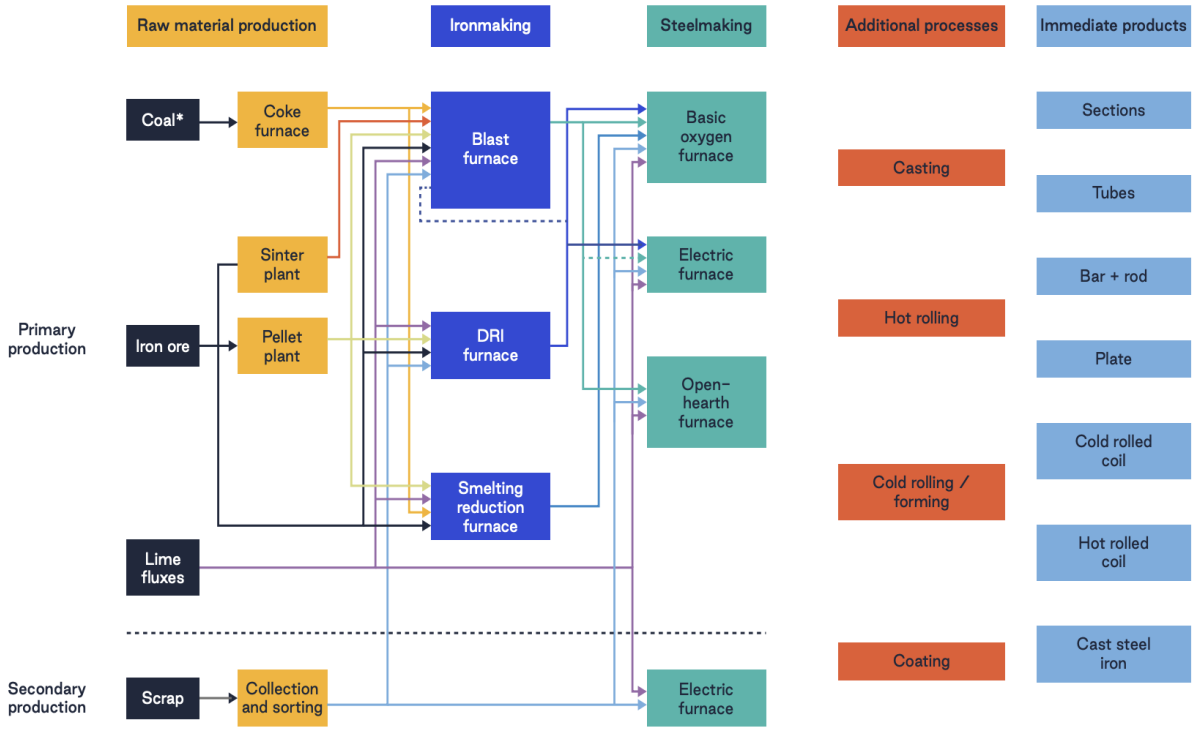

Figure 8 Source: Adapted from Cullen, et al (2021) and IEA (2020).

7.3. Appendix 2: Example of production estimates derived from satellite data - Gary Steel, Indiana, USA

This section illustrates the processing steps to derive production estimates from satellite imagery. We use the example of Gary Steel works, Indiana, USA, where we identify 12 hotspots in the plant (i.e., blast furnaces, slag pit etc.; see Figure 3).

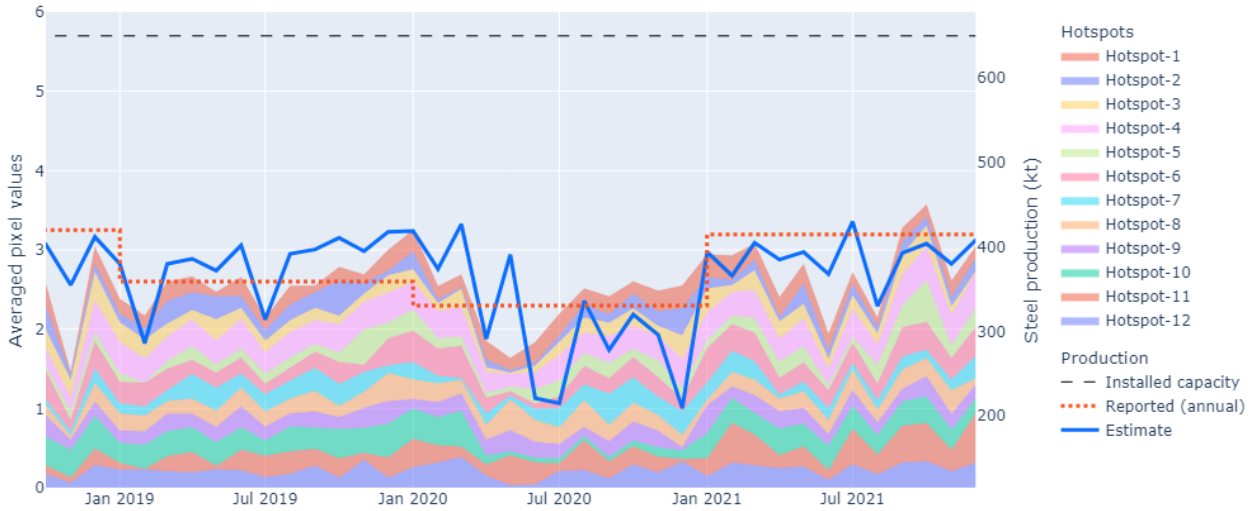

Figure 9 NHI values and production data for Gary Steel, Indiana, USA. Time series of averaged pixel values at each hotspot on the left axis. Reported production (red dashed line), NHI estimated production (solid blue line) and installed capacity (black dashed line) are shown on the right axis.

1. We start by extracting every pixel value from each image within the hotspots. Figure 9 shows the monthly average pixel values for each hotspot. At this stage it already shows a certain level of correlation with reported production.
2. We reduce dimensionality by applying a principal component analysis on the hotspots. The optimal number of principal components is derived through hyperparameter training (in the case of Gary steel, the optimal PCA is of one component).
3. We then normalise the reduced feature space between 0 and 1 by applying a MinMaxScaler.
4. This processed time series is then fed into the optimiser described in Figure 4, to derive the weights allowing the optimal conversion to tons of crude steel, while respecting the constraints (estimated production does not exceed installed capacity).

The advantages of this production estimation process become evident in Figure 9 whereby production values are provided at a monthly frequency (blue line) compared to the annual (red dashed line) frequency (in addition to being provided at only a monthly delay compared to annually). This improved granularity allows for greater insight into facility production rates. Gary Steel works could be described as functioning at approximately half capacity for 2019 and 2021 with fairly consistent production throughout the year. For 2020 however, a year marred by the pandemic many steel production facilities across the country operated at reduced capacity. This substantial drop in production is captured and reflected in our estimation.

7.4. Appendix 3: Example of the country-level coverage of steel production by modelling method - Germany

Germany is a country with a relatively large steel production capacity (48.1 Mt/a) and benefits from monthly country-level production data. According to the GEM database it has 18 assets. Of the assets, 8 are BF-BOF (Total of 28.4 Mt/a) allowing for production estimates to be approximated via satellite monitoring, the remaining 10 assets are EAF (Total of 19.7 Mt/a), and production is subsequently estimated via the capacity-based approach. In order to estimate facility level production, a model is first developed for the satellite-based assets and trained against a scaled (in accordance with capacity) country level reported data. The significance of each hotspot within each asset is a learned outcome, and their NHI variation over time is indicative of the production activity at a particular facility. Where satellite-based methodology allows for capturing of the variation in production for a particular facility and may vary accordingly, the remaining capacity-based asset production is estimated based on the difference in known country level production from the satellite production estimates. As such the production activity between capacity-based assets is proportional to one another. Lastly, the shortfall in country production by our estimates is attributed to the omission of small assets (<0.5 Mt/a) in the GEM database. This may occur when the accumulated capacity of the known assets is lower than the published country level production values. We account for this missing production via the introduction of a non-spatially allocated asset. The production estimates for each of these methodologies is expressed for Germany in Figure 10.

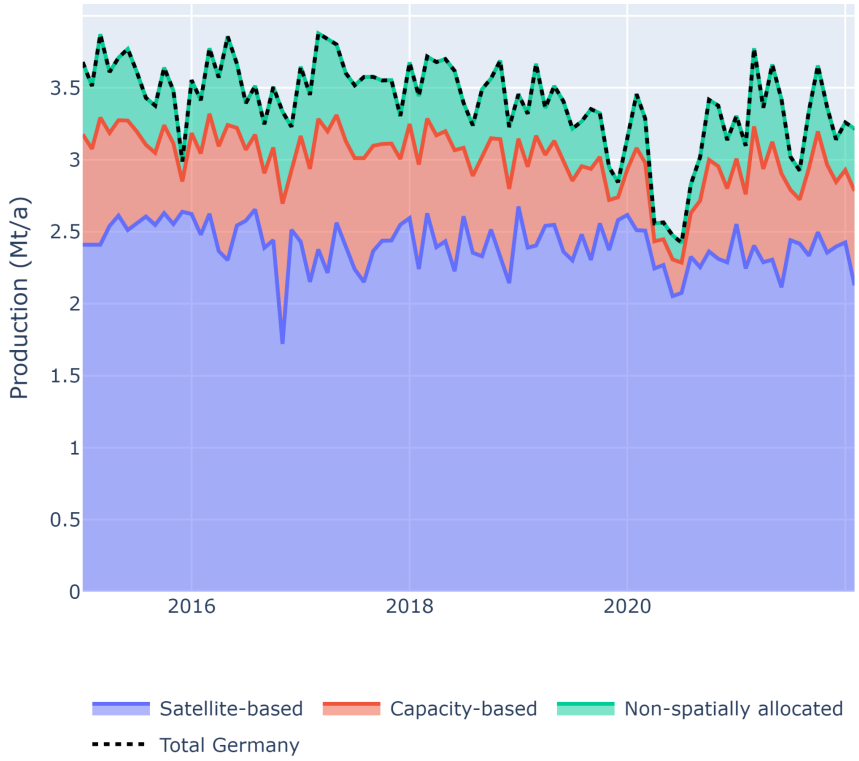

Figure 10 Asset type production estimates for Germany (2015-2022).

7.5. Appendix 4: Summary of the coverage by geographies (2021)

Table 2 Summary of the data coverage by country, with a breakdown of the steel plants monitored by satellite (expressed by number of assets, share of installed capacity, production and emissions). Values representative for 2021.

Country	Total assets	Satellite-monitored Assets	Total asset production (Mt)	Satellite-monitored production (Mt)	Total asset emissions ($MtCO_2$)	Satellite-monitored emissions ($MtCO_2$)	Total asset capacity (Mt)	Satellite-monitored capacity (Mt)
China	332	198 (60%)	818.3	672.0 (82%)	1225.1	1042 (85%)	1170.5	911.0 (78%)
Japan	39	15 (38%)	87.7	65.5 (75%)	131.3	122.7 (93%)	119.1	88.2 (74%)
United States	72	9 (12%)	85.8	22.9 (27%)	49.9	34.4 (69%)	116.2	36.7 (32%)
India	45	17 (38%)	71.2	43.8 (61%)	144.2	95.8 (66%)	123.8	89.8 (72%)
Russia	26	8 (31%)	66.1	49.1 (74%)	72	66.1 (92%)	84.4	62.4 (74%)
South Korea	15	3 (20%)	64.1	50.1 (78%)	85.6	82.6 (96%)	84.5	57 (67%)

Turkey	25	3 (12%)	40.4	10.5 (26%)	21.3	16.2 (76%)	53.7	13.3 (25%)
Germany	18	8 (44%)	35.4	28.4 (80%)	42.9	41.4 (96%)	48.1	36.3 (75%)
Brazil	22	7 (32%)	32.8	21.5 (65%)	43.1	35.5 (83%)	47.1	31.1 (66%)
Iran	18	2 (11%)	28.5	3.2 (11%)	10.3	4.2 (41%)	38.5	6.3 (16%)
Italy	23	1 (4%)	22.6	4.1 (18%)	11.3	7 (62%)	34.2	11.5 (34%)
Mexico	14	2 (14%)	18.5	7 (38%)	12.5	6.7 (54%)	25.7	12 (47%)
Vietnam	14	2 (14%)	18.5	9.3 (50%)	26.2	18.4 (70%)	24.9	13.1 (53%)
Ukraine	11	7 (64%)	17.1	13 (76%)	32.7	26.6 (81%)	42.3	34.4 (81%)
Taiwan	5	2 (40%)	15.5	5 (32%)	21.8	6.8 (31%)	19	7.1 (37%)
Spain	14	1 (7%)	14.2	0.9 (7%)	7.6	1.3 (17%)	19.1	1.2 (6%)
Indonesia	6	2 (33%)	13.7	6.5 (47%)	17.7	10.6 (60%)	13.7	6.5 (47%)
France	10	2 (20%)	13.1	9 (68%)	17	16 (94%)	19.8	11.9 (60%)
Canada	8	3 (38%)	11.1	6.3 (57%)	10.5	8.3 (79%)	15.5	9.8 (63%)
Egypt	7	1 (14%)	10.3	0.3 (3%)	2.9	0.5 (16%)	14.9	2.1 (14%)
Saudi Arabia	6	0 (0%)	8.7	0 (0%)	3.1	0 (0%)	14.6	0 (0%)
Poland	6	1 (17%)	7.4	3.8 (52%)	9.3	8.3 (90%)	11.4	5 (44%)
Malaysia	10	0 (0%)	6.9	0 (0%)	4.9	0 (0%)	14.1	0 (0%)
Austria	2	2 (100%)	6.4	6.4 (100%)	10.4	10.4 (100%)	7.6	7.6 (100%)
Netherlands	1	1 (100%)	6.4	6.4 (100%)	10.5	10.5 (100%)	7.5	7.5 (100%)
United Kingdom	5	2 (40%)	6.3	5.7 (91%)	9.5	9.3 (99%)	11	8.1 (74%)
Belgium	4	1 (25%)	5.9	4.4 (74%)	7.5	7.1 (95%)	8.1	5 (62%)
Thailand	8	0 (0%)	5.5	0 (0%)	1.3	0 (0%)	7.6	0 (0%)
Argentina	4	1 (25%)	4.7	2.3 (49%)	4.3	3.7 (87%)	6.9	3.2 (47%)
Australia	4	2 (50%)	4.7	3.8 (80%)	6.4	6.2 (96%)	5.8	4.4 (76%)

Algeria	3	0 (0%)	4.2	0 (0%)	2.4	0 (0%)	7.7	0 (0%)
Czech Republic	2	2 (100%)	4.1	4.1 (100%)	6.7	6.7 (100%)	6.2	6.2 (100%)
Sweden	5	2 (40%)	4.1	3 (73%)	5.2	4.9 (95%)	5.8	3.8 (65%)
Finland	3	1 (33%)	3.9	2.2 (58%)	4	3.6 (90%)	4.7	2.6 (56%)
Bangladesh	5	0 (0%)	3.7	0 (0%)	0.9	0 (0%)	4.8	0 (0%)
Slovakia	2	1 (50%)	3.6	3.6 (100%)	5.8	5.8 (100%)	5.1	4.5 (88%)
South Africa	4	2 (50%)	3.4	2.5 (74%)	4.3	4.1 (95%)	8.4	6.4 (77%)
Romania	4	1 (25%)	3.3	2.2 (65%)	3.8	3.6 (93%)	5.2	3 (58%)
United Arab Emirates	1	0 (0%)	2.9	0 (0%)	0.7	0 (0%)	3.5	0 (0%)
Kazakhstan	1	1 (100%)	2.6	2.6 (100%)	4.3	4.3 (100%)	6	6 (100%)
Belarus	1	0 (0%)	2.4	0 (0%)	0.6	0 (0%)	3	0 (0%)
Luxembourg	2	0 (0%)	2.1	0 (0%)	0.5	0 (0%)	3.5	0 (0%)
Oman	4	0 (0%)	2	0 (0%)	0.5	0 (0%)	6.8	0 (0%)
Pakistan	4	1 (25%)	1.8	0 (0%)	0.4	0 (0%)	5.4	3 (56%)
Serbia	2	1 (50%)	1.7	1.5 (92%)	2.5	2.5 (99%)	2.7	2.2 (81%)
Greece	4	0 (0%)	1.5	0 (0%)	0.4	0 (0%)	6.6	0 (0%)
Hungary	3	1 (33%)	1.3	1.2 (94%)	2	2 (99%)	2.8	1.6 (56%)
Portugal	2	0 (0%)	1.3	0 (0%)	0.3	0 (0%)	1.7	0 (0%)
Kuwait	1	0 (0%)	1.2	0 (0%)	0.3	0 (0%)	1.2	0 (0%)
North Korea	5	3 (60%)	1.2	1 (84%)	1.7	1.4 (81%)	10.7	9 (84%)
Chile	2	1 (50%)	1	0.8 (79%)	1.4	1.4 (96%)	2	1.5 (74%)
Bosnia and Herzegovina	1	1 (100%)	0.9	0.9 (100%)	1.3	1.3 (100%)	1.9	1.9 (100%)
Qatar	1	0 (0%)	0.9	0 (0%)	0.2	0 (0%)	2.6	0 (0%)

Uzbekistan	1	0 (0%)	0.9	0 (0%)	1.4	0 (0%)	1	0 (0%)
Libya	1	0 (0%)	0.7	0 (0%)	0.2	0 (0%)	1.8	0 (0%)
Moldova	1	0 (0%)	0.6	0 (0%)	0.1	0 (0%)	1	0 (0%)
Norway	1	0 (0%)	0.6	0 (0%)	0.1	0 (0%)	0.7	0 (0%)
Slovenia	1	0 (0%)	0.6	0 (0%)	0.1	0 (0%)	0.7	0 (0%)
Bulgaria	1	0 (0%)	0.5	0 (0%)	0.1	0 (0%)	1.4	0 (0%)
Morocco	2	0 (0%)	0.5	0 (0%)	0.1	0 (0%)	1.8	0 (0%)
New Zealand	1	0 (0%)	0.5	0 (0%)	0.1	0 (0%)	0.7	0 (0%)
Peru	2	0 (0%)	0.5	0 (0%)	0.8	0 (0%)	1.6	0 (0%)
Singapore	1	0 (0%)	0.4	0 (0%)	0.1	0 (0%)	0.8	0 (0%)
Switzerland	1	0 (0%)	0.4	0 (0%)	0.1	0 (0%)	0.7	0 (0%)
Guatemala	1	0 (0%)	0.3	0 (0%)	0.1	0 (0%)	0.5	0 (0%)
Philippines	1	0 (0%)	0.3	0 (0%)	0.1	0 (0%)	0.5	0 (0%)
Azerbaijan	1	0 (0%)	0.2	0 (0%)	0	0 (0%)	1	0 (0%)
Albania	1	0 (0%)	0.1	0 (0%)	0.1	0 (0%)	0.7	0 (0%)
Nigeria	3	0 (0%)	0.1	0 (0%)	0.1	0 (0%)	3.6	0 (0%)
Latvia	1	0 (0%)	0	0 (0%)	0	0 (0%)	0.9	0 (0%)
Syria	2	0 (0%)	0	0 (0%)	0	0 (0%)	2.2	0 (0%)
Trinidad and Tobago	1	0 (0%)	0	0 (0%)	0	0 (0%)	1	0 (0%)
Venezuela	1	0 (0%)	0	0 (0%)	0	0 (0%)	5.1	0 (0%)

Table 3 Summary of the coverage in Chinese provinces, with a breakdown of the steel plants monitored by satellite in the coverage (expressed by number of assets, share of installed capacity, production and emissions). Values representative for 2021.

Chinese province	Total assets	Satellite Assets	Total production (Mt)	Satellite production (Mt)	Total emissions ($MtCO_2$)	Satellite emissions ($MtCO_2$)	Total capacity (Mt)	Satellite capacity (Mt)
Hebei	66	47 (71%)	207.6	169.6 (82%)	318.3	263.5 (83%)	291.5	217.7 (75%)
Jiangsu	31	20 (65%)	103.7	97 (94%)	157.7	150.1 (95%)	129.2	113.6 (88%)
Liaoning	14	11 (79%)	58.1	54.8 (94%)	89.8	85.1 (95%)	74.7	68.6 (92%)
Shandong	22	18 (82%)	55	49.7 (90%)	84.6	77.2 (91%)	83.1	73.5 (88%)
Shanxi	23	19 (83%)	53.6	43.5 (81%)	83.3	67.7 (81%)	78.9	63.8 (81%)
Guangxi	17	3 (18%)	33.2	12.5 (38%)	43.6	19.4 (45%)	49.8	21.1 (42%)
Hubei	16	3 (19%)	27.9	16.9 (60%)	38	26.2 (69%)	39.5	23.6 (60%)
Henan	16	11 (69%)	26.8	23 (86%)	40.6	35.8 (88%)	45.2	37.9 (84%)
Anhui	9	7 (78%)	26.7	25.4 (95%)	40	38.5 (96%)	35.7	33.7 (94%)
Guangdong	9	4 (44%)	23.8	18.1 (76%)	33.2	28.2 (85%)	35.7	26.4 (74%)
Fujian	13	5 (38%)	19.8	11.6 (58%)	28.1	18 (64%)	29.6	16.9 (57%)
Inner Mongolia	9	6 (67%)	19.3	16.5 (85%)	30	25.6 (85%)	29	25.3 (87%)
Yunnan	11	7 (64%)	17	12.4 (73%)	25.4	19.2 (76%)	24.3	17.4 (71%)
Sichuan	8	3 (38%)	16.9	11.6 (69%)	23.8	18 (76%)	22.2	15.4 (69%)
Tianjin	9	4 (44%)	16.4	13.7 (84%)	25.4	21.4 (84%)	33.1	22.4 (68%)
Jiangxi	5	4 (80%)	16.1	15.5 (96%)	24.5	24.1 (98%)	22	21 (95%)
Hunan	4	3 (75%)	14.6	13.6 (93%)	22.6	21.1 (93%)	20.6	19.3 (94%)
Shanghai	2	1 (50%)	14.4	14.2 (99%)	22.2	22.1 (99%)	17.7	16.2 (92%)
Zhejiang	8	2 (25%)	10	6.9 (69%)	13.2	10.8 (82%)	14.2	9 (63%)
Xinjiang	8	5 (62%)	9.7	7.7 (79%)	13.5	11.9 (88%)	16.9	12.8 (76%)
Jilin	8	4 (50%)	9.5	7.4 (78%)	13.6	11.6 (85%)	16.3	12.4 (76%)

Shaanxi	4	3 (75%)	8.7	7.9 (91%)	12.5	11.9 (95%)	13.5	12.3 (91%)
Gansu	3	2 (67%)	8.3	7.6 (92%)	12.7	11.8 (94%)	11.6	10.5 (91%)
Chongqing	4	1 (25%)	7.9	6.8 (86%)	11.7	10.5 (90%)	11.4	8.4 (74%)
Heilongjiang	3	3 (100%)	5.7	5.7 (100%)	8.9	8.9 (100%)	8	8 (100%)
Guizhou	8	0 (0%)	5.2	0 (0%)	4.1	0 (0%)	13.2	0 (0%)
Qinghai	1	1 (100%)	1.5	1.5 (100%)	2.4	2.4 (100%)	2	2 (100%)
Ningxia	1	1 (100%)	0.9	0.9 (100%)	1.4	1.4 (100%)	1.8	1.8 (100%)

7.6. Appendix 5: Accuracy results for selected assets and years between 2015 and 2021.

Table 4 Model accuracy for the 22 assets with known target production and emissions. For assets with multiple samples the average is shown (median sample rate = 2).

Asset ID	Asset name	Geography	Main production process	Capacity (Mt/a)	Implied emissions factor	Production (Mt/a) MAE (MAPE)	Emissions ($MtCO_2/a$) MAE (MAPE)
SCZ00001	Provozovna Třinec	Czech Republic	BF-BOF	2.6	1079	0.52 (26%)	0.53 (16%)
SES00008	ARCELORMITTAL ESPAÑA - PLANTA SIDERÚRGICA DE AVILÉS Y GIJÓN	Spain	BF-BOF	4.2	1618	0.17 (6%)	0.93 (26%)
SFR00002	ARCELORMITTAL FOS	France	BF-BOF	5.1	1975	0.03 (1%)	0.68 (11%)
SIT00003	ArcelorMittal Italia	Italy	BF-BOF	11.5	1372	0.05 (1%)	1.46 (20%)
SLU00001	ArcelorMittal Belval & Differdange S.A.	Luxembourg	EAF	2	137	0.02 (1%)	0.12 (42%)
SLU00002	ArcelorMittal Belval & Differdange S.A.	Luxembourg	EAF	1.5	219	0.02 (3%)	0.02 (11%)
SPL00002	TAMEH POLSKA sp. z o. o. - Zakład Wytwarzania Kraków (Elektrociepłownia)	Poland	BF-BOF	2.6	942	0.43 (26%)	2.43 (68%)
SUS00003	CLEVELAND-CLIFFS STEEL CORPORATION DEARBORN WORKS	United States	BF-BOF	3	694	0.46 (21%)	1.99 (61%)
SUS00004	AK Steel Corporation - Middletown	United States	BF-BOF	3	2237	0.26 (15%)	1.51 (57%)
SUS00005	CLEVELAND-CLIFFS RIVERDALE LLC	United States	BF-BOF	1	239	0.08 (13%)	0.83 (84%)
SUS00006	Cleveland-Cliffs Burns Harbor LLC	United States	BF-BOF	5	2065	0.1 (3%)	2.28 (39%)
SUS00007	CLEVELAND-CLIFFS PLATE LLC-COATESVILLE	United States	EAF	0.8	591	0.38 (61%)	0.01 (8%)
SUS00008	Cleveland-Cliffs Steelton LLC	United States	EAF	1	669	0.64 (81%)	0.1 (53%)

SUS00009	Cleveland-Cliffs Steel LLC	United States	BF-BOF	7.25	1258	0.5 (10%)	0.94 (13%)
SUS00010	Cleveland-Cliffs Cleveland Works LLC	United States	BF-BOF	4.1	1577	0.29 (11%)	0.34 (8%)
SUS00016	SSAB ALABAMA INCORPORATED	United States	EAF	1.27	315	0.13 (14%)	0.11 (46%)
SUS00017	SSAB Iowa Inc.	United States	EAF	1.13	436	0.12 (14%)	0.21 (102%)
SUS00046	TIMKENSTEEL CORP (1576000613)	United States	EAF	1.11	524	0.39 (45%)	0.04 (17%)
SUS00047	US Steel (Edgar Thomson)	United States	BF-BOF	2.7	1763	0.17 (8%)	0.23 (7%)
SUS00049	US Steel Corp - Gary Works	United States	BF-BOF	7.8	1939	0.37 (8%)	2.27 (34%)
SUS00051	US STEEL - GRANITE CITY	United States	BF-BOF	2.8	1773	0.44 (27%)	0.4 (16%)
SUS00059	NLMK INDIANA	United States	EAF	0.77	169	0.05 (7%)	0.04 (26%)